Int J Adv Manuf Technol (2018) 95:1265–1280
https://doi.org/10.1007/s00170-017-1300-3

ORIGINAL ARTICLE

Microstructural and tribological behavior of in situ synthesized Ti/Co coatings on Ti-6Al-4V alloy using laser surface cladding technique

O. S. Adesina [1] · A. P. I. Popoola [1] · S. L. Pityana [2] · D. T. Oloruntoba [3]

Received: 21 August 2017 / Accepted: 1 November 2017 / Published online: 9 November 2017

Abstract The enhancement of the tribological properties of titanium (Ti-6Al-4V) has been the subject of wide range research over the years. The constraints associated with Ti-6Al-4V in severe tribological conditions due of its low hardness and poor wear properties can be enhanced by appropriate enhancement of the microstructure via surface modification technique without altering the bulk material. In this work, Cp-Ti and Co powders were deposited at different admixed percentages by laser cladding on Ti-6Al-4V substrates with respect to laser processing parameters. The laser optimized parameters used are laser power 900 W, powder feed rate 1.0 g/min, beam spot size 3 mm, and gas flow rate 1.2 L/min while scan speed were varied at 0.6and 1.2m/min. The microstructural evolution as well as wear morphology of the coatings were studied using scanning electron microscope equipped with energy dispersed spectrometry (SEM/EDS) while the phase identification were observed using X-ray diffractometer (XRD). Microhardness values of the coatings were obtained while wear test was conducted using a reciprocating set up. The coatings exhibited a good metallurgical bonding between the coatings and the substrate. Results revealed that laser clad sample with high scan speed was more effective in improving the hardness and wear resistance of Ti-Co/Ti6Al4Vcompared to low scan speed. The coatings possess an average hardness value of 730 $HV_{0.1}$, a value that is about two times greater than that of the substrate. The enhanced wear resistance with high laser scan speed has been attributed to the presence of flower-like structures and formation of fractions of $CoTi_2$, CoTi, $AlTi_2$, $AlCo_5$, $AlCo_2Ti$, and Al_2Ti inter-metallic phases dispersed within the coating matrix. In addition, analysis of worn surfaces and wear mechanism indicated improved resistance to tribological actions.

Keywords Laser cladding technique · Cp Ti-Co powders · Intermetallic phases · Microstructure · Tribological behavior and Ti6Al4V

1 Introduction

Titanium and its alloys as a kind of distinctive metallic materials have been extensively used in engineering fields such as in aerospace structures, heat exchangers, and offshore platforms owing to their wide ranging performances attributed to unique high strength-to-weight ratio and corrosion resistance [1–3]. However, the main setback of Ti–6Al–4V consists in its poor tribological characteristics including high friction coefficient and fretting wear resistance [4–6]. According to Chikarakara et al. [7], titanium alloys are often characterized by the problems of surface wear via adhesive and abrasive mechanisms, and subsurface damage through plastic deformation from contact loading. Each time an engineering component is in motion with another contacting component, the contacting surfaces are exposed to both friction and wear. Therefore, the need for high hardness and wear resistance for the surface remains an essential factor. It has been stated that the wear resistance could be enhanced via surface modification provided a strong adhesion is achieved between the coating and the substrate [8]. In addition, surface modification can

✉ O. S. Adesina
osaadesina@yahoo.com

[1] Department of Chemical and Metallurgical Engineering, Tshwane University of Technology, P.M.B. X680, Pretoria 0001, South Africa

[2] Council for Scientific and Industrial Research (CSIR) – National laser Centre, P.O. BOX 395, BLD 46F, Pretoria 0001, South Africa

[3] Department of Metallurgical and Materials Engineering, Federal University of Technology, Akure, P.M.B. 704, Akure, Ondo, Nigeria

also be used in reducing coefficient of friction as well as enhance surface hardness by altering the surface microstructure of materials but retaining the composition of the bulk material [9]. Various surface modification techniques employed in improving surface properties of titanium and its alloy includes nitriding, thermal oxidation, chemical vapor deposition, and plasma electrolytic oxidation [10–13]. Today, numerous researches have been made to enhance the wear resistance of Ti alloys by the use of laser surface cladding technique [14, 15]. Laser cladding is a fast solidification process in which a laser beam is employed as heating source to fuse powder or alloys with a substrate [1, 16, 17]. The process is characterized by several unique advantages such as high cooling rate, little dilution ratio, a crack-free layer, limited heat affected zone, a dense coating, and strong metallurgical bonding to substrate [18–21].

Co-containing alloys are extensively used in the industry for sliding wear application [22, 23]. This is due to the fact that cobalt has strong precipitation hardening effect on titanium alloys owing to the development of diffuse Ti_2Co hard precipitates during aging process [24]. Also, cobalt powders are widely considered in tribological-related applications because of their intrinsic high strength properties and ability to maintain hardness over a wide temperature range [25]. Although, Co-containing coatings play a significant role in enhancing surface properties of titanium alloys. Nevertheless, challenges such as differences in the thermo-physical properties between the cladding materials like Co and the titanium alloy substrates might prompt formation of cracks and porous clad layers [26]. Fortunately, laser cladding with the use of optimized processing parameters can eradicate these aforementioned defects [27, 28]. It is noted that surface properties of the laser coatings mainly depend on laser processing parameters such powder flow rate, scanning velocity, and laser power [29]. In fact, scanning velocity has major significant effect on the resultant microstructures [30, 31].

Literatures establish significant enhancement in microhardness and wear resistance of titanium alloy as a result of the presence of intermetallic coatings such as CoTi, $TiCo_3$, and Ti_2Co [25, 32, 33]. These intermetallic compounds are of importance owing to their high hardness, better oxidation resistance, phase stability, and good mechanical properties [26]. The works of Dutta Majumdar et al. [32] and XUE et al. [33] stated that the microstructure was found to be refined with a dense microstructure comprising of mainly primary dendrites structures which grew in the opposite direction of the heat flow.

However, exploiting the need for development of complex microstructures and novel in situ intermetallic phases from admixed ratio of Ti and Co elemental powders that will enhance the said limitation of Ti alloy is the motivation for this research. From the best of the authors' knowledge, there is no information on influence of admixture and scan speed on laser surface cladded Ti-6Al-4V with TiCo. In this present work, the scope is to study the influence of admixed CpTi/Co and laser scanning speed on the microhardness, hardness, and tribological properties of Ti-6Al-4V. The work is considered to provide profound insight and contribute detailed knowledge of the effect of laser parameters on material performance. Furthermore, comprehensive study on microstructural evolution and its influence on coefficient of friction and wear morphology of the coatings were carried out.

2 Experimental details

2.1 Materials and process

Titanium and cobalt elemental powders (both of 99.9% purity, 45–90 μm) supplied by TSL Germany was used as feedstock powders in the present study. The morphological characteristic of the powders was examined using scanning electron microscopy (SEM) fortified with energy dispersive spectrometer (EDS). The SEM images of the two as-received powders are presented in Fig. 1a, b. The titanium and cobalt powders were observed to be round and sphere-shaped with satellites, a predictable characteristic associated with atomized powders. A comparable outcome was described by Zhu et al. [34]. A 200-ml tubular vessel was filled with powders and placed in the mixing chamber. The powders were blended via turbula mixer at a speed of 300 rpm for 6 h. This is to achieve homogeneity which is of great significance to enhance flowability and to prevent inhomogeneous mixture caused by powder agglomeration which may perhaps cause irregular flowability of the powders [35].

Ti-6Al-4V plates were used as substrates (50 × 50 × 5 mm) with a chemical composition shown in Table 1. The plates (substrate) were sandblasted by spraying them with SiO_2 grit sand and cleaned with acetone prior to laser cladding process. This was aimed at obtaining clean and uniform surfaces which help to minimize reflection of laser radiation as well as enhance absorption of laser energy at the surface of the titanium alloy [36].

2.2 Laser processing

Laser surface cladding was employed to deposit admixed powders on Ti-6Al-4V plates using a continuous wave 4.4 kW RofinSinarNd:YAG laser. The clad powders (pure commercial titanium and cobalt) were infused in an admixed proportion into the melt pool formed by the laser beam during scanning of the substrate. The cladding tracks were formed by varying sets of parameters to optimize the power and the scan speed. The laser optimization parameters were as follows: laser power 900 W, powder feed rate 1.0 g/min, beam spot size 3 mm, gas flow rate 1.2 L/min, and different scan speeds

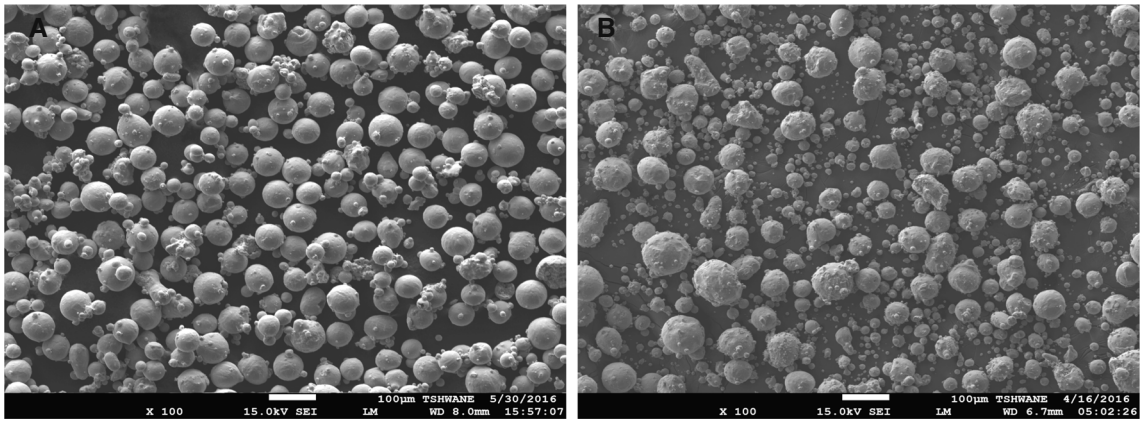

Fig. 1 SEM morphology of the as-received **a** titanium and **b** cobalt powders

of 0.6 and 1.2 m/min. The précised relationship between the process parameters and the composition of admixed powders is shown in Table 2. In the course of laser cladding process, the molten pool was protected by argon gas flowing at 3 L/min. This was done in order to prevent oxidation as Ti has high affinity for oxygen. In order to produce laser coatings with large surface area, multiple tracks were obtained at 50% overlap at an angle of 45 degree to the substrate.

2.3 Characterization of laser coatings

After laser cladding process, coatings for microstructural characterization were grinded and polished using diamond suspension. Thereafter, the polished samples were etched in kroll's reagent for approximately 10 s. Scanning electron microscope (SEM) was used to study the cross-section morphologies of the laser clad coatings while qualitative elemental compositions were revealed by energy dispersive spectroscopy (EDS) (FE-SEM JSM-7600F). The phases were examined using Philips PW1713 X-ray diffractometer (XRD) fitted with monochromatic CuKα radiation set at 40 Kv and 20 mA, while phase identification was done using Philips Analytical X'Pert High Scores software fitted with an in built (ICSD) database. The scan was taken between $10^{o}$and 80^{o} 2 theta (2θ) and a step size of 0.02^{o}.

2.4 Hardness test

Vickers hardness test was carried out on the cross-sectioned layers of the cladded samples using Vickers hardness Tester EMCOTEST. Vickers hardness profile indentations were taken at a load of 100 gf (0.98 N) with dwelling time of 15 s on the surface of the cladded area towards the substrate. Thereafter, with five different indentations at neighboring regions on the clad surface, an average value was calculated for each specimen. This is subsequently performed on the free surface of the coating and also, along the longitudinal plane of each sample.

Table 1 Chemical composition of Ti6Al4V (wt.%)

Ti	Al	V	Fe	C	O	N
Balance	6.10	4.01	0.15	0.007	0.12	0.005

2.5 Tribological test

Tribological tests were performed on deposited Ti6Al4V coatings using UMT–2–CETR tribometer under reciprocating sliding conditions with constant recording of coefficient of friction values. This device allows forward and backward sliding where the friction coefficient of both strokes are measured. Samples of dimensions 2 × 2 cm were set in a sample holder while load were applied vertically downward on the specimens. The motor-driven carriage applies a load sensor for feedback to maintain a constant applied load. A normal load of 15 N at a frequency of 5 Hz, sliding velocity of 2 m/s, 2 mm sliding distance, and 1000 s of reciprocating movement were used. The experimental results indicating wear depth and coefficient of friction were obtained using the CERT UMT-2 tribometer software. The worn surfaces were observed under scanning electron microscope (SEM) in order to study the features of the worn surfaces after the dry sliding wear test and investigate possible wear mechanism.

3 Results and discussion

3.1 Coating dimension

The SEM images of the laser clad 60Ti–40Co coatings on Ti6Al4V substrate are shown in Fig. 2. Dense and well compacted coatings were fabricated on the substrate exhibiting strong metallurgical bond between the laser coating and the substrate. In addition, the coatings displayed microstructures with no inclusion of cracks, defects or pores. It is

Table 2 Laser processing parameters

Sample	Clad material	Power (W)	Scan speed (m/min)	Beam diameter (mm)	Powder feed rate (g/min)	Gas flow (L/min)
1	60%Ti – 40%Co	900	0.6	3	1.0	1.2
2	60%Ti – 40%Co	900	1.2	3	1.0	1.2
3	40%Ti – 60%Co	900	0.6	3	1.0	1.2
4	40%Ti – 60%Co	900	1.2	3	1.0	1.2

observed that the coating thickness of the coating cladded at a lower scan speed (Fig. 2a) shows larger build-up with wider dilution zone compared to the coating deposited at a scan speed of 1.2 m/min (Fig. 2b). This discrepancy can be associated with the lengthened period of powder deposition and simultaneous interaction between the laser beam and the melt pool. In effect, there is a larger gradient of migration and fusion of the coating particles into the topmost layers of substrate, yielding a larger region of interfacial dilution. According to Mahamood et al. [37], at lower scan velocity, increased laser and substrate interaction results to more energy density, therefore sustains dwelling period of the melt pool on the substrate. This supports proper mixing of powders and formation of novel phases within the melt pool. This phenomenon is also exhibited in Fig. 3, representing 40Ti–60Co coatings deposited at 0.6 m/min (Fig. 3a) and 1.2 m/min (Fig. 3b). The rough surfaces observed on the coatings indicate unmelted or partially melted particles of the powders deposited. A rationale behind this effect is the high convective influence on laser surface processing which disallows complete dissolution of the powders at free surfaces except at temperatures far higher than the melting point of the powders [38]. The undulating pattern of the coatings is associated with the mode of deposition of multiple tracks as maximum deposition is situated at the center of each track. In reference to Figs. 2 and 3, it could be observed that at lower scan speed, the build-up for 60Ti–40Co coatings deposited showed 927 and 464 μm at high scan speed while the build-up at lower scan speed for 40Ti–60Co coatings showed 1.01 mm and 546 μm at high scan speed.

3.2 Coating matrix

The matrix of 60Ti-40Co coating is reported in Fig. 4. Figure 4a is portrayed by equal fraction of light gray primary dendrites enriched with Ti and inter-dendritic Co-rich eutectics reflecting a dark gray coloration [39]. Possible compounds that can be contained in this structure are CoTi and $CoTi_2$ [24, 40]. The primary dendrites appear as coarse polygonal flakes owing to well-developed overlapping secondary dendritic arm width. Figure 4b shows the microstructural morphology of coating deposited at 1.2 m/min. The matrix of the coating is characterized with needle-like (acicular) structures coupled with appreciable secondary arms in the upper region while a leaf-like structure is observed at the lower region of the matrix. It could be said that the rate of energy loss within the coating matrix is high leading to inadequate growth of the dendritic width and secondary arms. Furthermore, the length of the primary dendrites indicates a preferred crystal growth direction and the rapid transition of heat as solidification takes place.

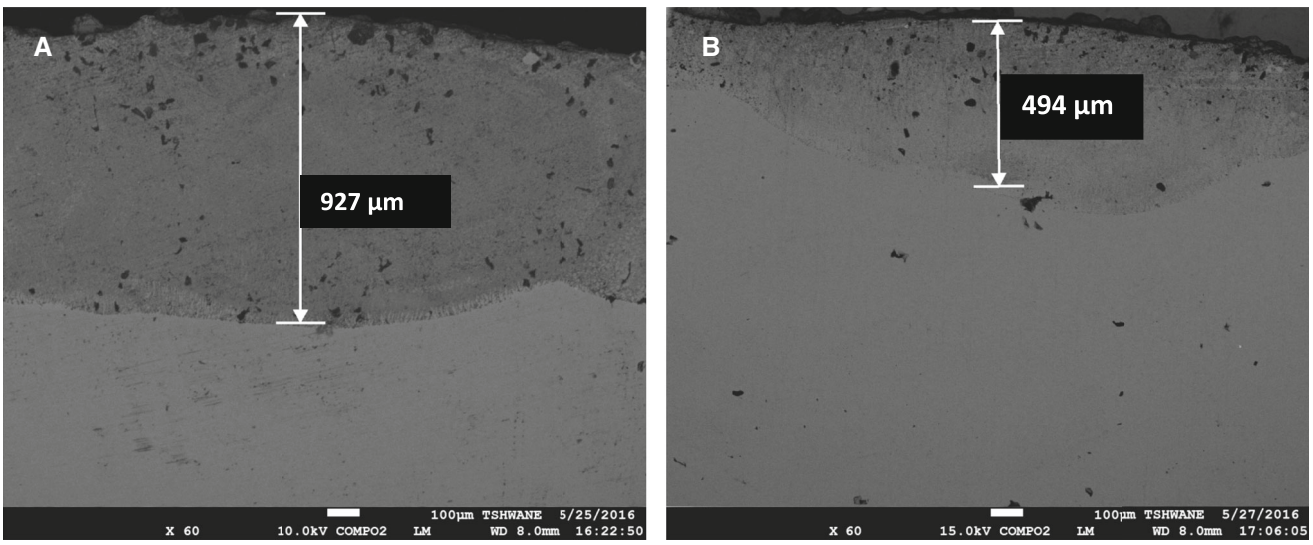

Fig. 2 Micrograph of cross sectional view of 60Ti /40Co coating at **a** 0.6 m/min and **b** 1.2 m/min

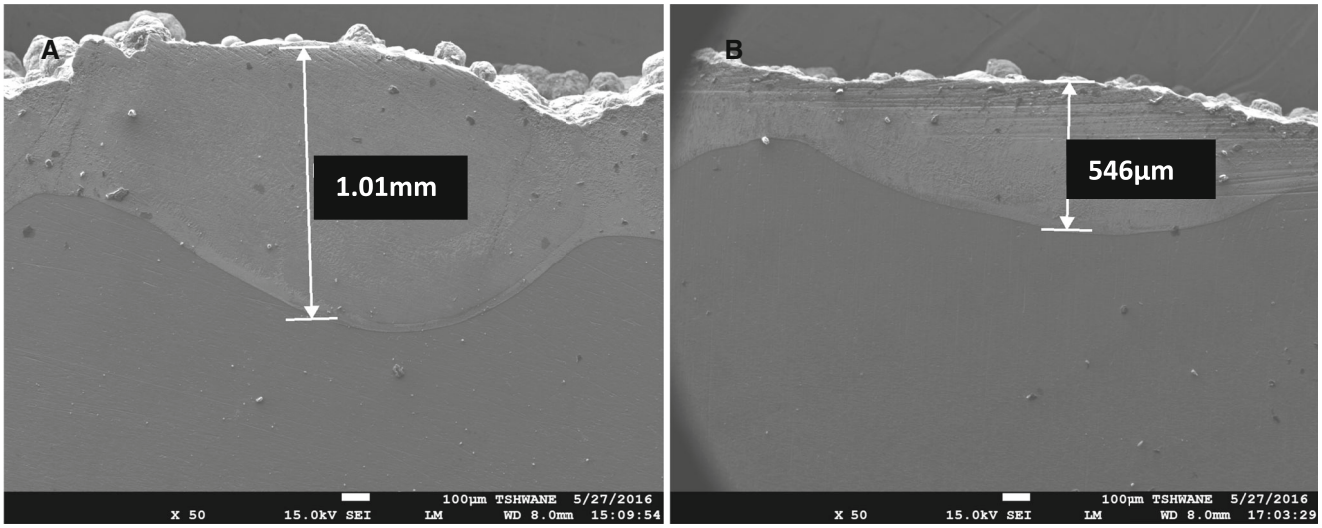

Fig. 3 Micrograph of cross sectional view of 40Ti/60Co coating at **a** 0.6 m/min and **b** 1.2 m/min

Formation of flower-like dendrites mainly dominates the matrices of 40Ti-60Co intermetallic coatings presented in Fig. 5. The SEM images exhibit flower-like dendritic patterns across the matrix of the coatings at different laser scan speeds. As more percentage of cobalt is incorporated, there is a support for formation of cobalt rich intermetallic phase Co_3Ti which might be as a result of a subtle but rapid atomic repositioning during solidification, propelling the resultant dendritic structures. Considering further examination in Fig. 5, the solidification mechanism associated with lower scan speed is mainly governed by crystal growth while at higher scan speed, nucleation appears to possess the upper hand in affecting the morphology of the microstructure.

3.3 Interfacial zones

According to Fig. 6, the microstructure of the coating revealed good dendritic structures distributed in the matrix of metallic coatings. With respect to Fig. 6a, there is a shift from equiaxed grains situated at the middle region of the coating to unidirectional dendrites located at the transition zone. As solidification occurs, the direction of heat flow is multi-axial at the middle region of the coating, yielding a formation of equiaxed structures. Within the transition zone, columnar grains are observed, indicating a directional growth towards the substrate. Similar results were also reported by Meng et al. [41] and Weng et al. [42]. In summary, coating fabricated at higher scan speed produced longer needle-like columnar structures at regions near the heat affected zone. Higher scan speed is associated with increased rate of solidification due to the rapid transfer of heat from the melt pool to the surrounding regions, causing the near-interfacial regions to attain a larger amount of dendritic formation. On the other hand, at low laser scan speed of 0.6 m/min, the clad layer transits to a larger dilution region, relating to a longer energy supply from the heat source to support mixing and material transport between the coating and the substrate. This is line with the observation of Alemohammad et al. [26] and Damborenea [43].

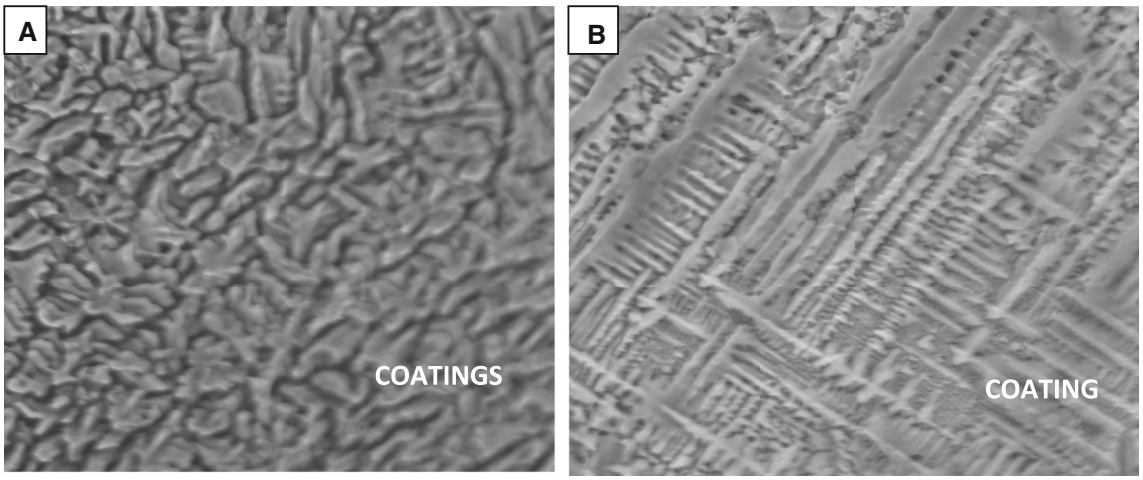

Fig. 4 SEM images of 60Ti-40Co coatings at **a** 0.6 m/min and **b** 1.2 m/min

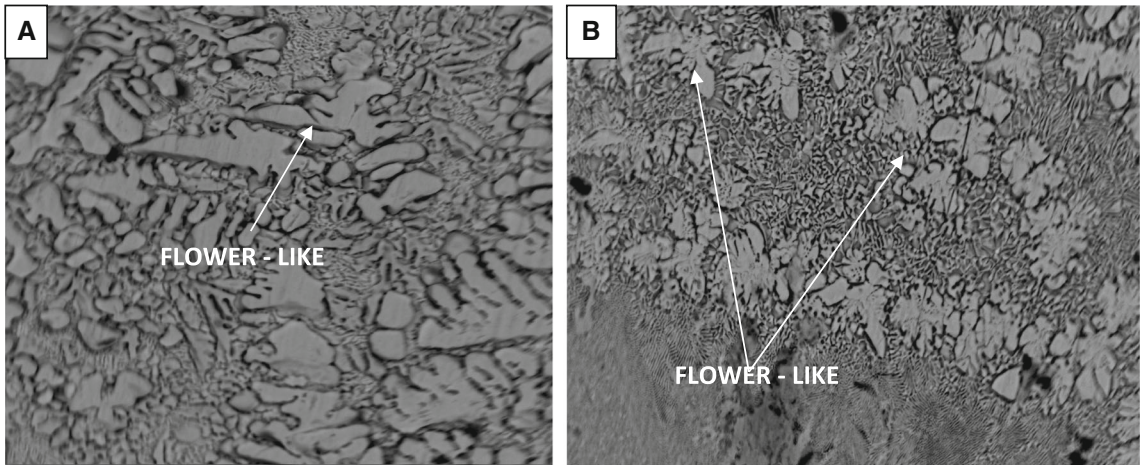

Fig. 5 SEM images of 40Ti-60Co coatings at **a** 0.6 m/min and **b** 1.2 m/min

With respect to the EDS presented in Fig. 6, the higher peak of aluminum in 6(a) indicates a higher dilution of the coating by the substrate, while silicon appears as trace element. In the EDS analysis, titanium shows the largest peak as this clearly indicates the large amount of titanium present both in the coating and the substrate. Furthermore, with lower laser scan speed, increased interaction time between the laser beam and the melt pool supports even distribution of deposited particles within the melt pool and, also a rise in the degree of melting.

Larger dendrites are observed in an aligned pattern towards the direction of heat flow in Fig. 7a. This suggests the sufficient time allowed by low scan laser scan speed during deposition, for complete melting of deposited powder and ordered growth in solidification. Placing this mode of solidification in

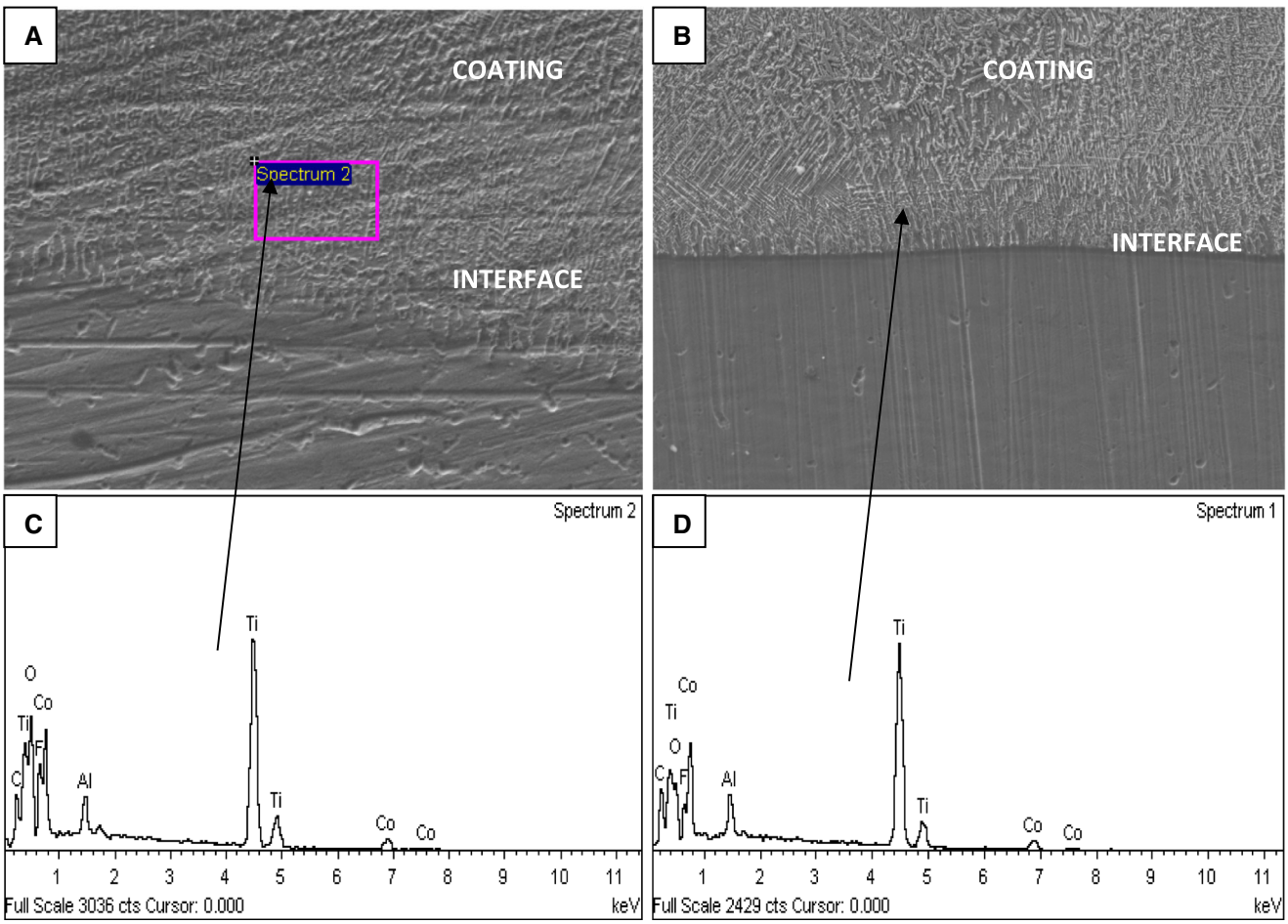

Fig. 6 SEM/EDS showing interfacial zone between coatings of 60Ti-40Co clad samples at **a** 0.6 m/min and **b** 1.2 m/min

comparison with the solidification achieved in Fig. 7b, secondary dendritic arm growth is limited and also, the growth is multi-directional. Higher dendritic formation characterized by 40Ti- 60Co coatings, in comparison with 60Ti- 40Co coatings, can be associated with the lower melting point of the more abundant powder, yielding an increased formation of secondary phases within the coating matrix. As laser source can supply heating effect of temperatures of about 2500 to 3200 °C to the coating surface and laser processing is associated with a rapid heating and cooling rate over a few millimeters of coating, powders that undergo ricocheting reduce the deposition efficiency as well as the heating efficiency, while fraction of the energy is lost to convective and radiative effects. Nevertheless, the absorbed energy can still maintain temperatures that are capable of completely melting the powders within the coating and producing theses secondary phases. The EDS in Fig. 7c, d exhibits higher peaks of cobalt compared to EDS analysis in Fig. 6, as a result to the higher percentage of cobalt within the coating.

3.4 XRD pattern analysis

Laser surface cladding supports the formation of diverse non-equilibrium phases with respect to its localized heating and self-sufficient rapid cooling of the melt pool. The various phases indicated in the XRD patterns shown in Figs. 8, 9, 10, and 11 are results of chemical reactions birthed in the molten pool via the effect of highly generated energy from laser beam on the cladding material and the substrate. This is in line with the study reported by Gordani et al. [44]. These phases present are the in situ compounds responsible for improved hardness and enhanced tribological properties. According to Rotella et al. [45], material melting that follows laser irradiation influences surface recrystallization and a broadening of the peaks present as new compounds are formed. It could be observed that no single oxide of aluminum, titanium, and cobalt was revealed in the XRD results. These benefiting from the non-interaction of the melt pool with the environment due to effective shielding by argon gas. The presence of oxide phases may lead to weak surface due to poor interfacial bonding [46]. It was observed that at both scan speeds, the Co-Ti ratio produced more major high diffraction peaks of $CoTi_2$. It has been reported by Xue et al. [33] that the presence of intermetallics of CoTi and a substantial amount of $CoTi_2$ produce excellent wear resistance. This might have been attributed to the inherent good toughness, high recrystallization temperature, and strong atomic bond of CoTi [32]. Majumdar et al. [32] investigated the properties of cladding that was fabricated using direct laser cladding of cobalt on Ti-6Al-4V. The wear was improved due to the combination of $CoTi_2$ and CoTi phases and α -Ti phases. The intermetallic compounds of Ti and Co attribute to the improvement of the wear resistance of the interface. In this work, it was observed that some compounds of aluminum were present, which is an indication of longer dwelling time of laser radiation and solidification at the melt pool. Further reaction was seen to have occurred with respect to the coatings deposited at different scan speeds (0.6 and 1.2 m/min). This could have resulted from the migration of aluminum present in the substrate at regions near the coating/substrate interface, reacting with Co-Ti, present in the coating, to form novel compounds of Al_5Co_3. Also, the prolonged release of energy from the laser beam could have promoted the transport and intense reactive actions of large mass fractions of titanium and cobalt atoms to the interface, aiding strong bonding at the interface. Although, $AlCo_2Ti$ was not displayed in the XRD analysis of 40C0-60Ti coatings, novel phases $AlTi_3$ and Co_3Ti were observed in the cobalt based coatings. The formation of these novel phases could be responsible for the increased surface properties of the coatings compared with higher percentage of titanium within the coating (40%Co).

3.5 Microhardness

The microhardness profile along the longitudinal section of the coatings are compared and represented in Fig. 12. Clearly, the coatings improved the hardness of the titanium alloy substrate. The coatings possess an average hardness value of 730 $HV_{0.1}$, a value that is about two times greater than that of the substrate. The hardness values of coatings deposited at 0.6 m/min maintained a high value to a depth of approximately 900 μm. This indicates the thickness of the coating as higher deposition is experienced and also confirmed by SEM images of the coatings compared to the coating deposited at a higher laser scan speed (approx. 550 μm). The microhardness of the cladded region is observed to be higher while the lower portion of the coatings experienced a progressive reduction in hardness due to the dilution effect from the substrate. The microhardness of the transition zones for coatings deposited at higher scan speed maintained slightly higher values than the substrate as the depth increased from 600 μm to about 800 μm. Essential information associated to this observation is the ultra-chilling effect experienced by the HAZ during solidification. Multiple peaks of hard $CoTi_2$ are observed with other phases indicated in the XRD results. The presence of these hard phases induces a combination of strengthening effect within the coating that is responsible for the elevated hardness of the coating. The surface hardness of the coatings shown in Fig. 13 confirms the improvement in hardness of the titanium alloy as the coatings are incorporated. There is a slight rise in hardness with increasing laser scan speed [37, 47]. The formation of CO_2Ti with increased speed at 40%Co and formation of Co_3Ti with increased speed at 60% Co accounted for the increased surface properties displayed by the coatings. This can be strengthened by the work of Langelier and Esmaeili [24].

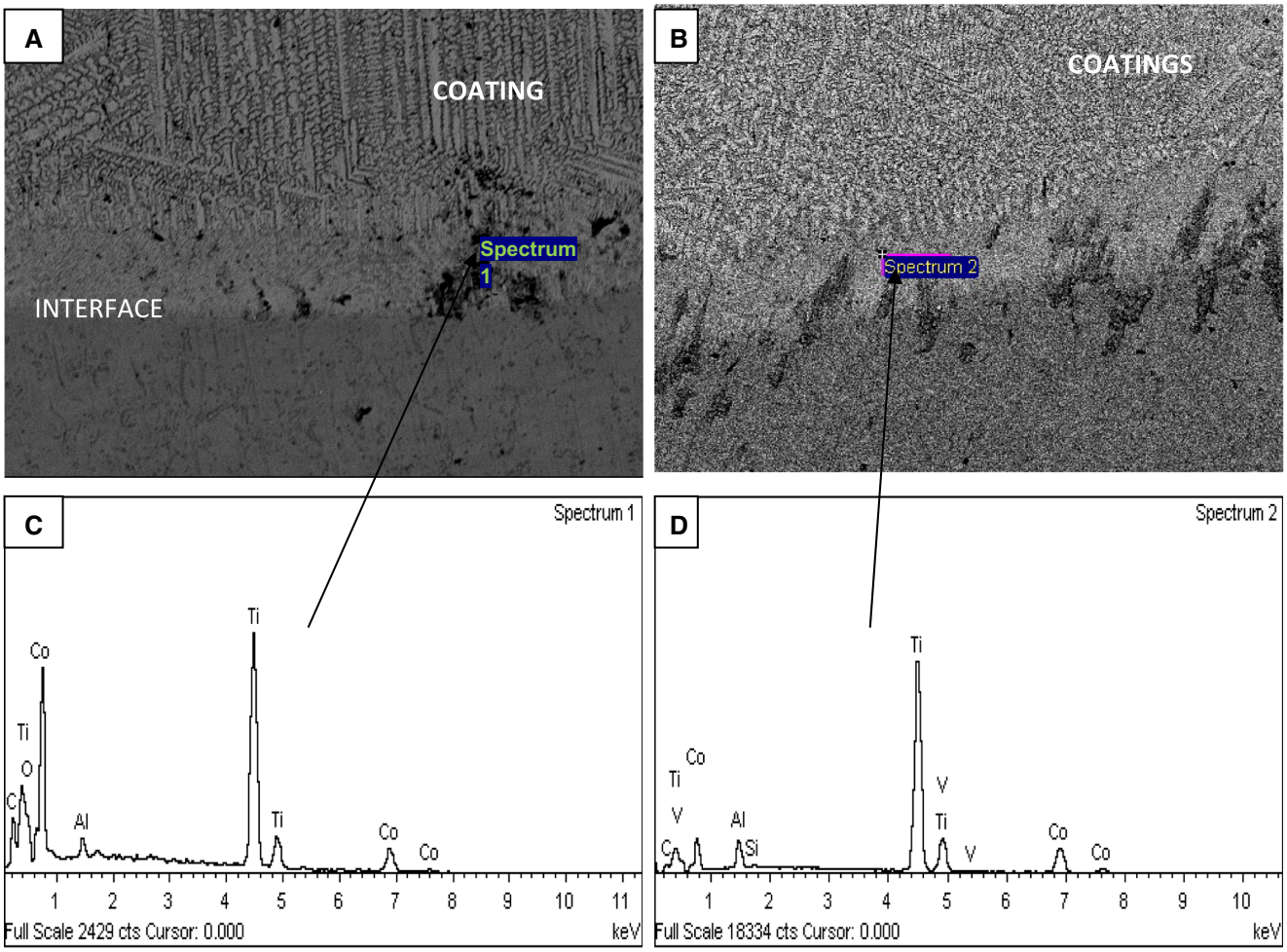

Fig. 7 SEM/EDS showing interfacial zone between coatings of 40Ti-60Co clad samples at **a** 0.6 m/min and **b** 1.2 m/min

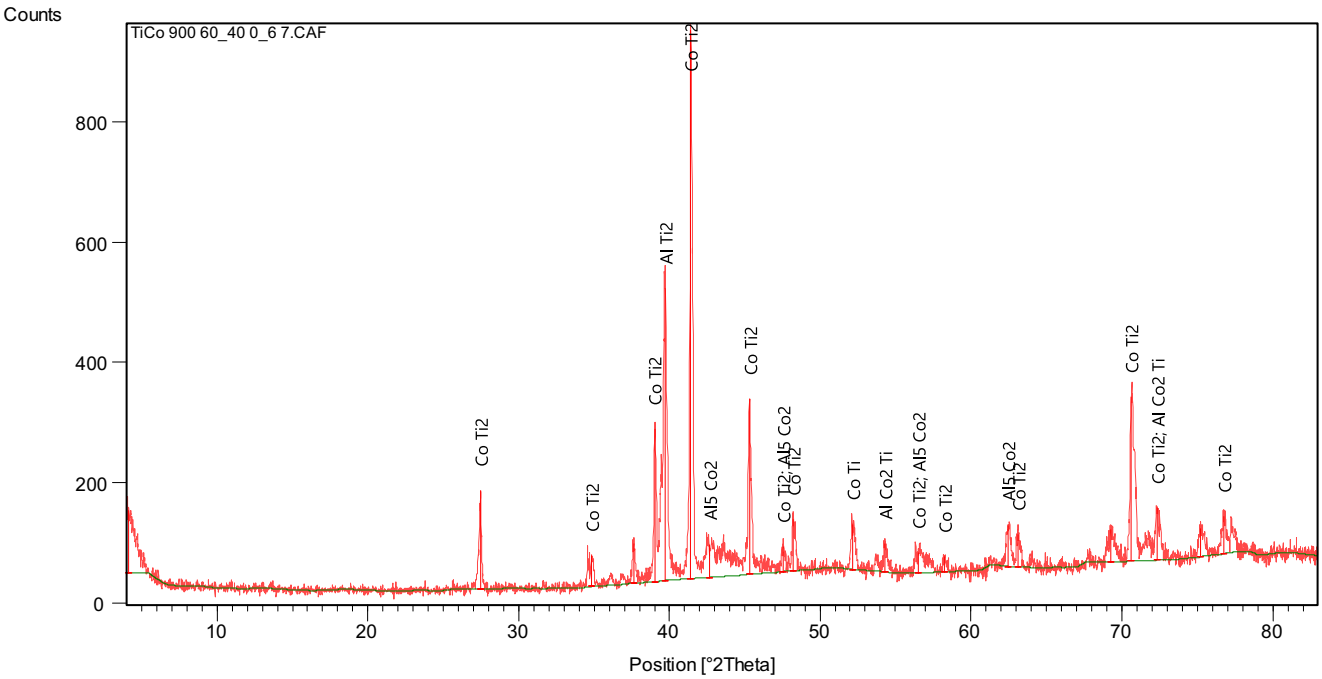

Fig. 8 XRD spectrum of laser clad 60Ti-40Co at 0.6 m/min

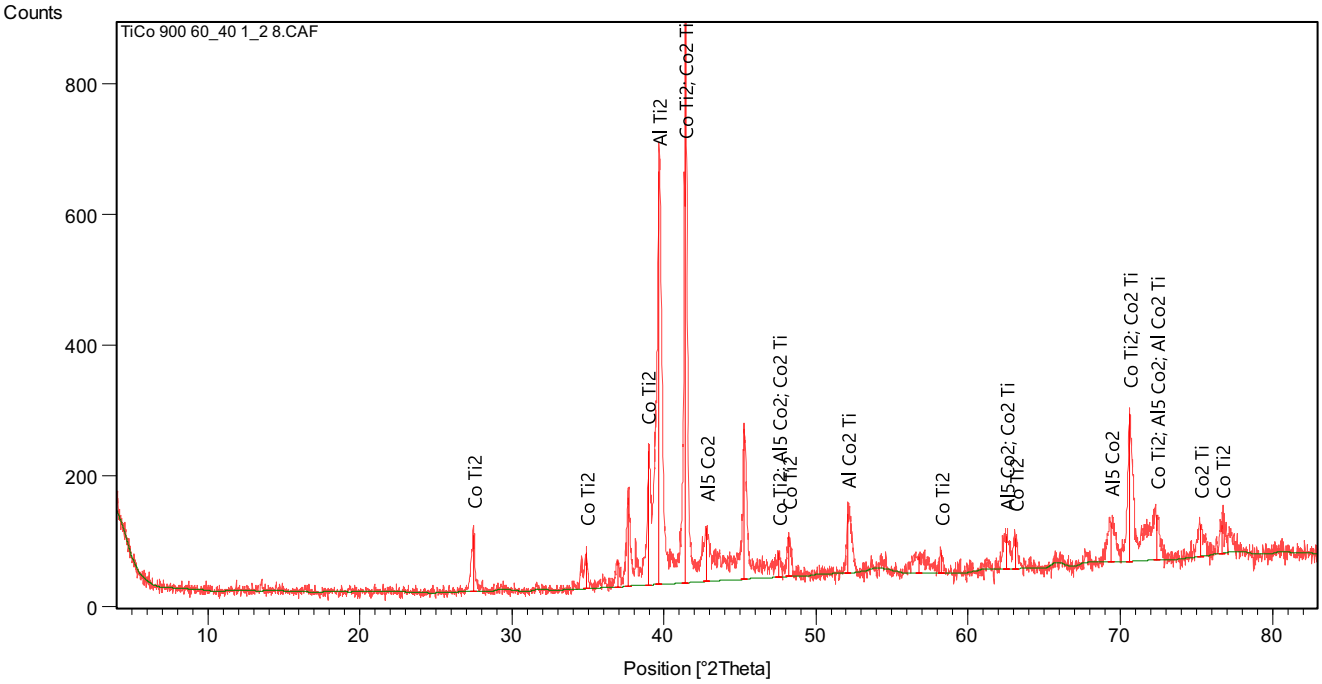

Fig. 9 XRD spectrum of laser clad 60Ti-40Co at 1.2 m/min

3.6 Wear scar morphology and mechanism

The worn surface of the substrate (Fig. 14 at different magnification) shows deep grooves into the surface of the sample. This could be due to low microhardness associated with Ti-6Al4-V, thereby causing the hard asperities on the surface of the honing wheel to easily penetrate into the substrate [4]. Equally, the presence of scratches, delamination of materials from the surface, and worn out debris were observed. With the parallel grooves observed, there is a distinctive clarity on the occurrence of abrasive wear mechanism. Figure 15 presents SEM images of wear scar of 60Ti-40Co metallic coatings. A smoother surface can be observed depicting an experience of a combination of abrasive mechanism with plastic deformation on the worn surface during the sliding dry test. Here, the wear process of TiCo/Ti-6Al-4V was similar to the observations by

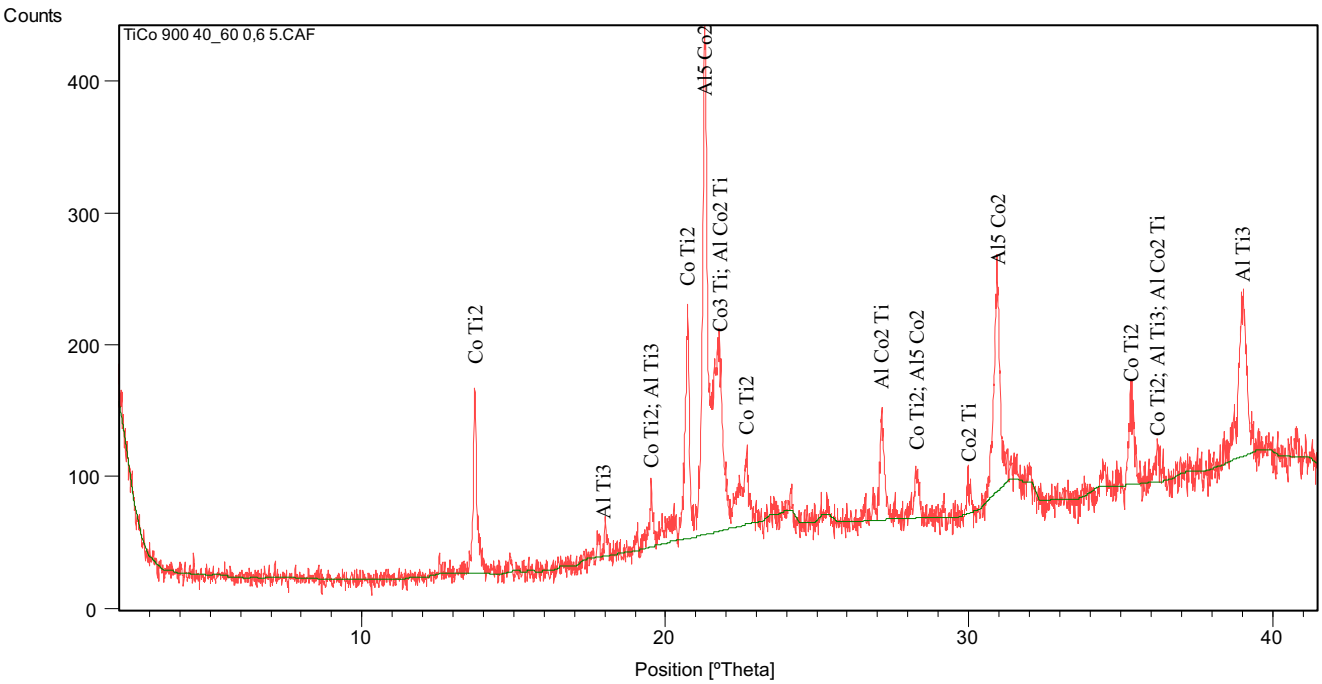

Fig. 10 XRD spectrum of laser clad 40Ti-60Co at 0.6 m/min

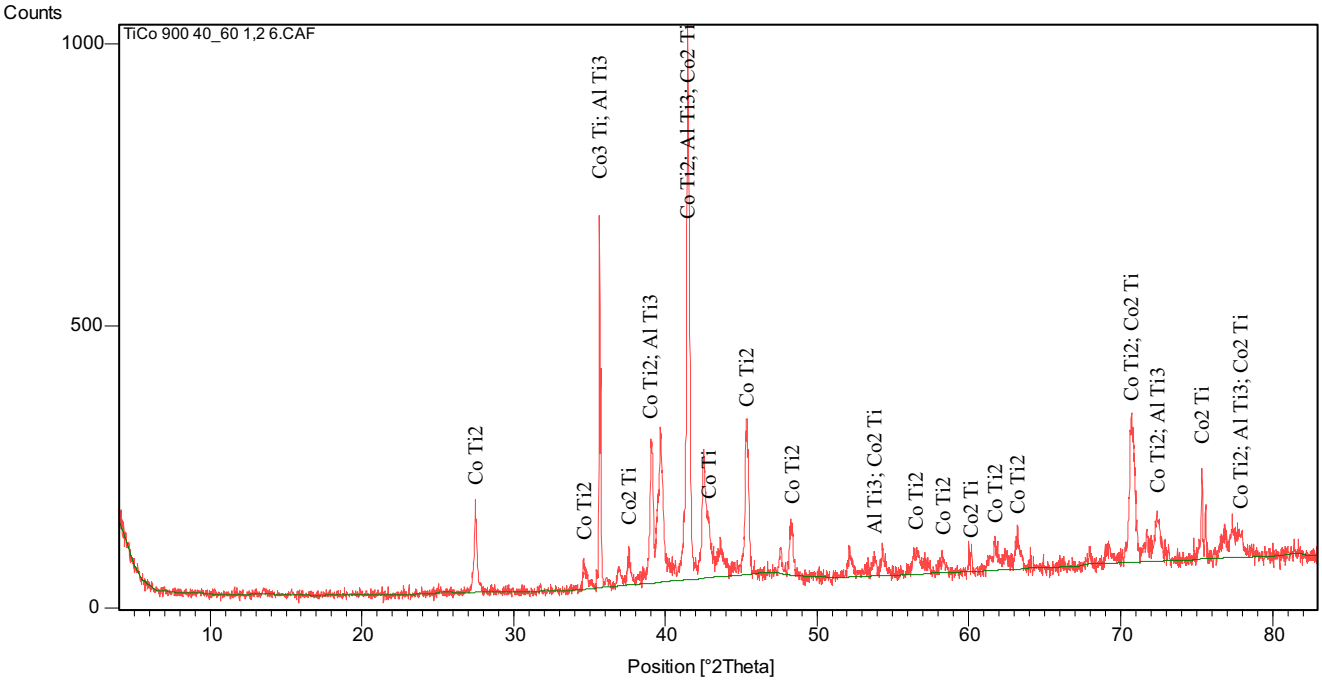

Fig. 11 XRD spectrum of laser clad 40Ti-60Co at 1.2 m/min

Li et al. [48], Ma et al. [49], and Xue and Wang [33]. Furthermore, surrounding regions of the wear grooves shown in Fig. 15a exhibiting the occurrence of plastic deformation mechanism. It could be seen that the surface is characterized with high level of plastic deformation and mild abrasive wear, when compared with the worn surface of the substrate in Fig. 14. This phenomenon was observed in the work of Cia et al. [50]. Micro hard intermetallic particles formed at the surface give rise to the increased gliding action. Figure 15c shows sparing amount of debris owing to possible uneven bonding of intermetallics within the surface of the coating. Tiny patches situated on the worn surface imply adhered debris smeared across the worn surface, observed at higher magnification (Fig. 15b, c). This infers the combined effect of mild plastic strain experienced between the sliding surfaces and high local temperature [51]. This order may also occur due to low hardness of 40% Co contained coatings compared to that of higher cobalt percentage as recorded in hardness properties.

Figure 16 shows the SEM images at a higher speed of 1.2 m/min. The worn surface observed appears to possess shallow grooves when compared with the morphology obtained in Fig. 15. A localized deposition of debris is observed along the shallow groove created by the steel ball. This localized deposition may arise from uneven micro-cutting as the asperities situated on the steel ball cascades along the sliding surface on the coating, portraying a typical pattern of mild abrasive wear mechanism. This report is in tandem with the work of Guo et al. [52]. The amount of the debris deposition on the worn surface of the coatings is much less than the

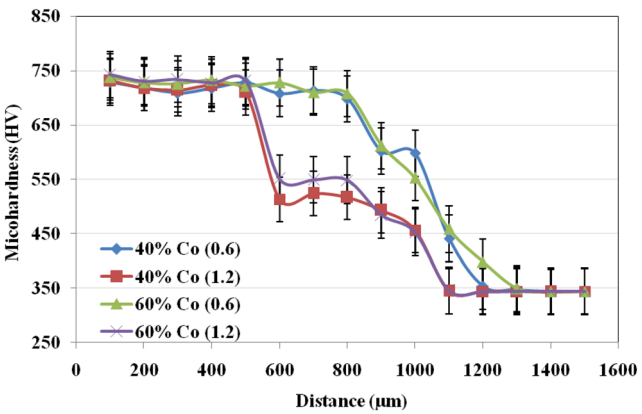

Fig. 12 Microhardness profile of TI-Co metallic coatings

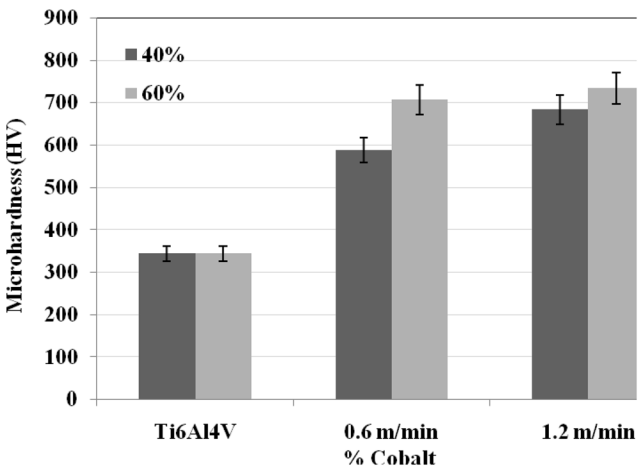

Fig. 13 Surface microhardness of TI-Co metallic coatings

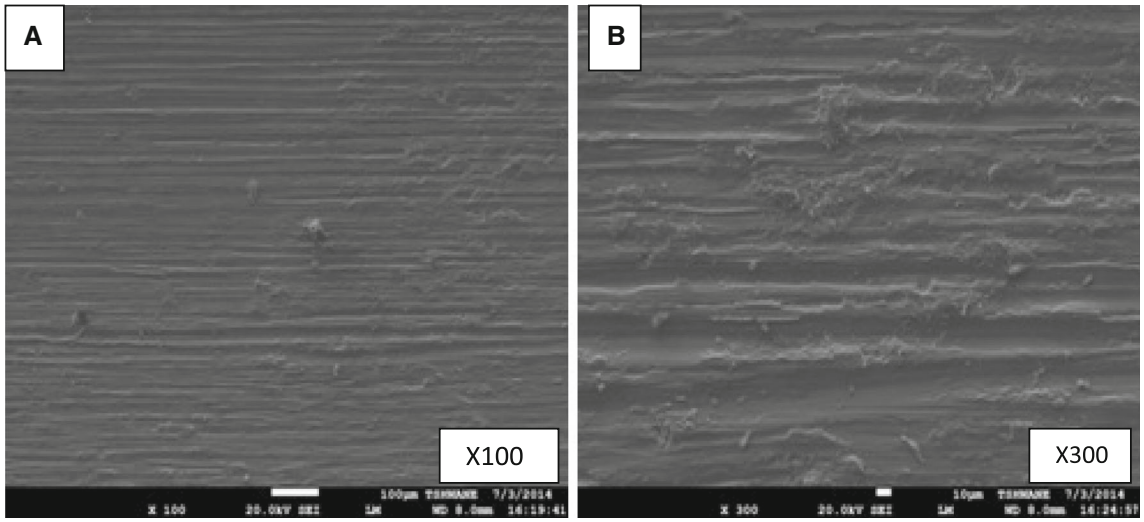

Fig. 14 SEM micrographs of worn surface morphology of substrate Ti-6Al4V **a** ×100 and **b** ×300

debris deposition of coatings fabricated at scan speed of 0.6 m/min which is observed to be virtually fused to the surface as a result of high local temperature, increasing the level of surface roughness; this may be a basis for development of interfacial

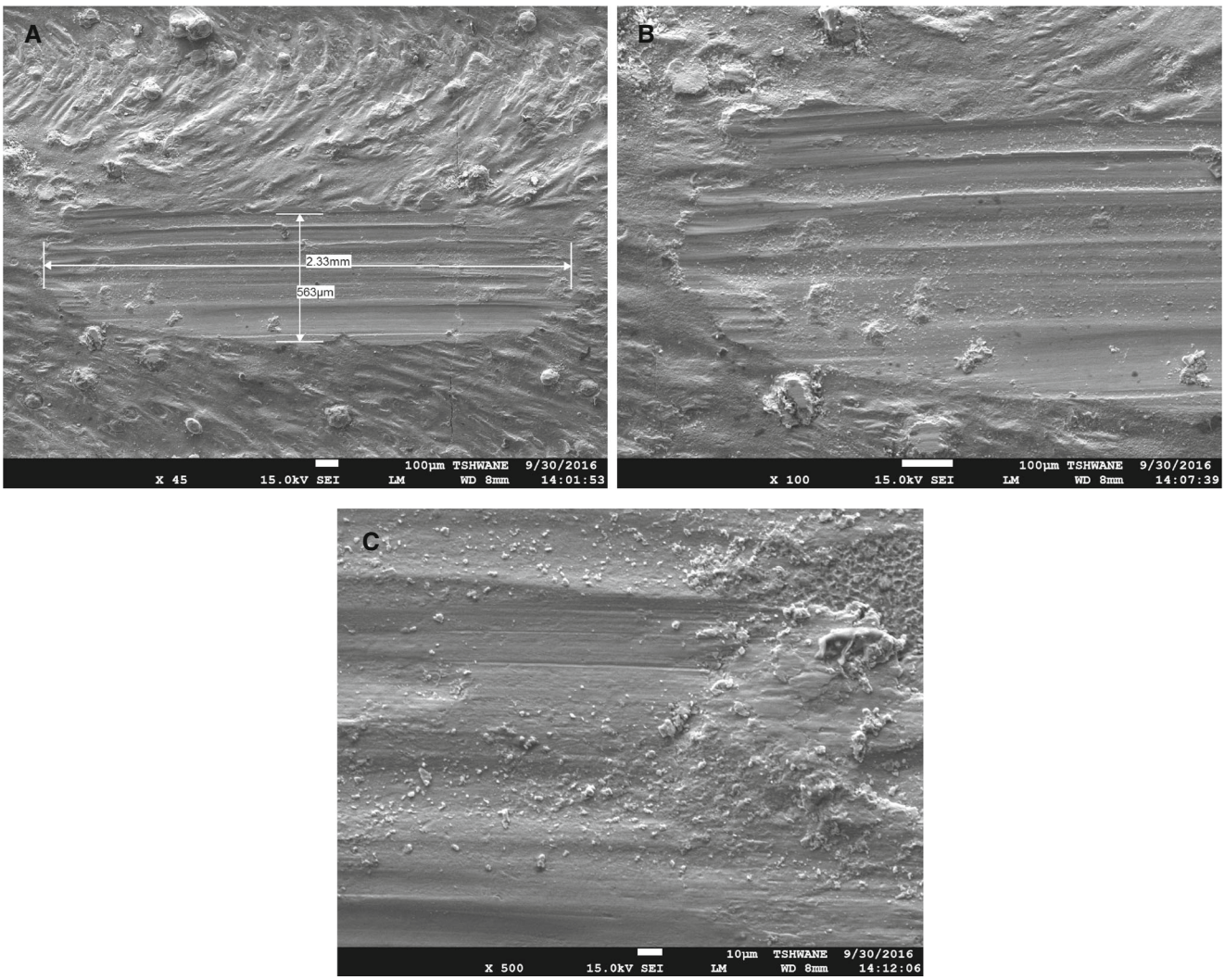

Fig. 15 SEM images of 60Ti - 40Co coatings at 0.6 m/min at **a** 40×, **b** 100×, and **c** 500× magnifications

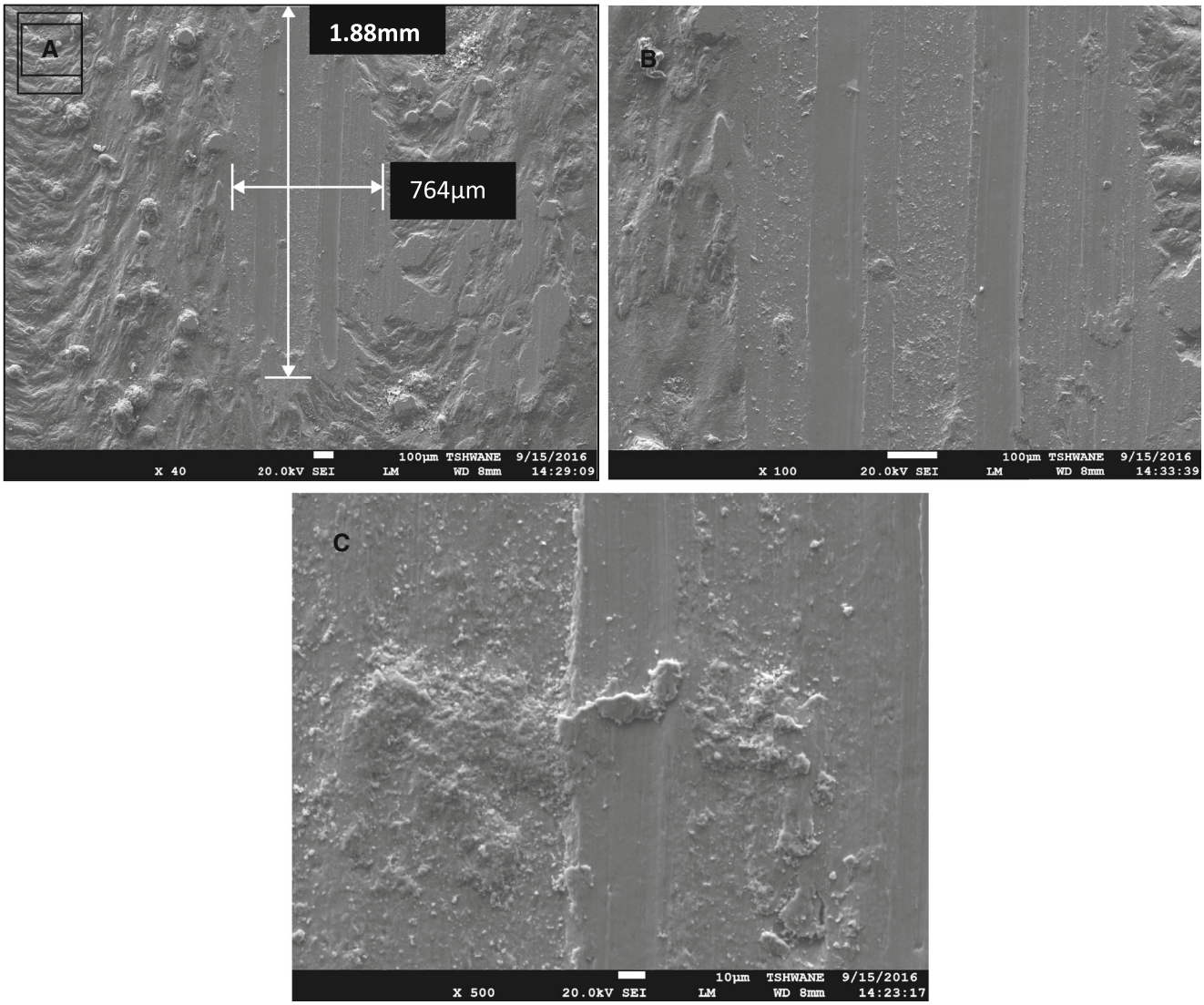

Fig. 16 SEM images of 60Ti - 40Co coatings at 1.2 m/min at **a** 40×, **b** 100×, and **c** 500× magnifications

stresses between the coating and the substrate. Also, coatings fabricated at higher laser scan speeds develop finer grains with stronger matrix, offering increased resistance to scratches or shear deformations. Hard asperities on the steel ball create shallow grooves on all the worn surfaces of the Ti-Co coatings as a result of good wear resistance of the coating surfaces.

In comparison, the effect of higher percentage of cobalt reinforcing particles is shown in Figs. 17 and 18. These parameters influence the wear mechanism(s) and affect the wear resistance of the coatings. It can be observed that wear scar is more severe in Figs. 15 and 16 compared to the micrographs in Figs. 17 and 18 displaying a better wear resistance. However, in Fig. 17b, there is an evidence of microstructural damage (crack) in the region close to the wear track. One hypothetical cause of this damage could be rapid increase in temperature caused from frictional forces during sliding test. The micro-cracks observed can also be linked with the formation of brittle cobalt-rich phases present within the coatings, generating an overall increase in brittleness of the coatings. Un-melted powders situated close to the worn surface undergo spalling effect as the honing steel slides across the surface. At higher laser scan speed a better wear resistance is observed (Fig. 18). It is also inferred that abrasive wear mechanism is the sole form of mechanism associated with the dry sliding test conducted on 40Ti-60Co coatings with minute material removal and high abrasion resistance.

3.7 Coefficient of friction

The variations in coefficient of friction with time of reinforced admixed laser clad metallic coatings and as-received Ti-6Al-4V alloy as substrate, under dry sliding situation of a load of 15 N is presented in Fig. 19. Evidently, the coefficients of friction of the metallic coatings are lower than that of the Ti-6Al-4V substrate, which was attributed to higher load bearing aptitude of CoTi, Al_5Co_3, $AlCo_5$, $AlCo_2Ti$, and $CoTi_2$ hard

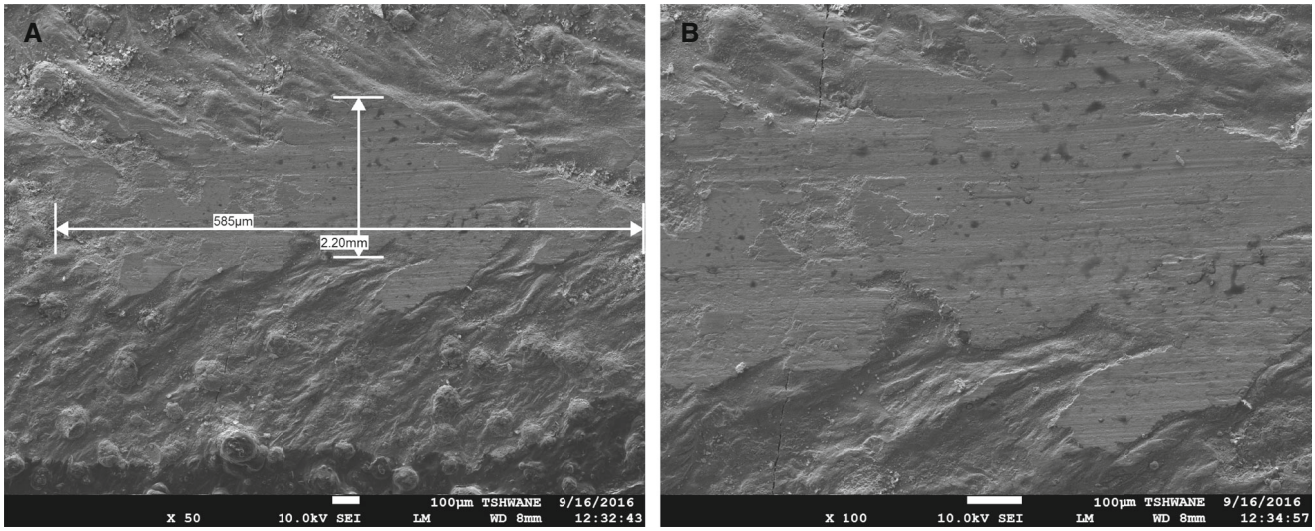

Fig. 17 SEM images of 40Ti - 60Co coatings at 0.6 m/min at different magnification

phases present in the coatings. The coefficients of friction of metallic coatings with higher cobalt percentage oscillate at the least level (below 0.18 μ) while coefficient of friction of metallic coatings with lower percentage oscillate at a level of about 0.18 to 0.26 μ. For a basis, higher laser scan speeds give rise to increased rate of solidification of laser deposited coatings which, in turn, produce matrices with smaller grain size. Consequently, the smaller the grain size the higher the resistance of the coating to deformation, which is according to the Hall-Petch equation [53]. Therefore, the reduced grain size of coatings with higher scan speeds enables the coatings to possess a reduced contact area of the coating surface with the steel ball, thus mitigating the smearing effect of the coatings on the steel ball. Also, more phases formed have yielded a more strengthening effect to the coating, reducing the potential surface enhancement.

3.8 Wear depth

The comparative wear depth analysis of worn surfaces of the control sample and the coatings subjected to dry sliding wear test is shown in Fig. 20. The metallic coatings demonstrate improved resistance to tribological actions as a result of well fused intermetallic phases, as well as enhanced coating adhesion and mechanical permanence of Ti and Co particles. Laser cladded 40Ti - 60Co coating at scan speed of 1.2 m/min shows the least amount of material removal owing to the increased rate of solidification to form stronger grains during laser processing, while 60Ti-40Co metallic coating fabricated at a speed of 0.6 m/min possesses a highest potency of material removal compared to other coatings but shows a better wear resistance than the control sample. Furthermore, it may be possible that during the dry

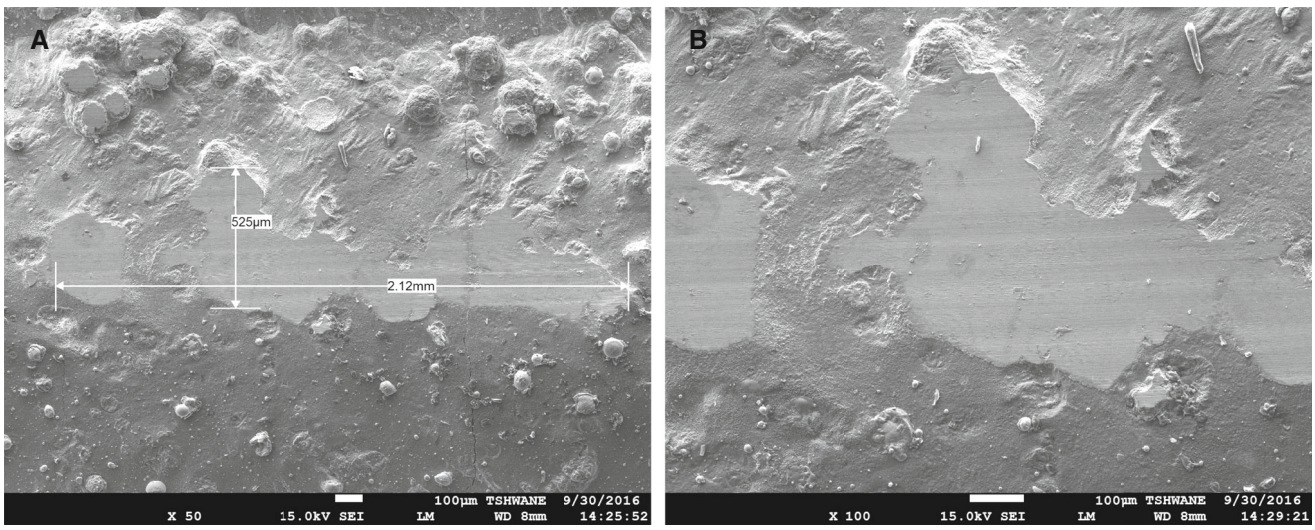

Fig. 18 SEM images of 40Ti - 60Co coatings at 1.2 m/min at different magnification

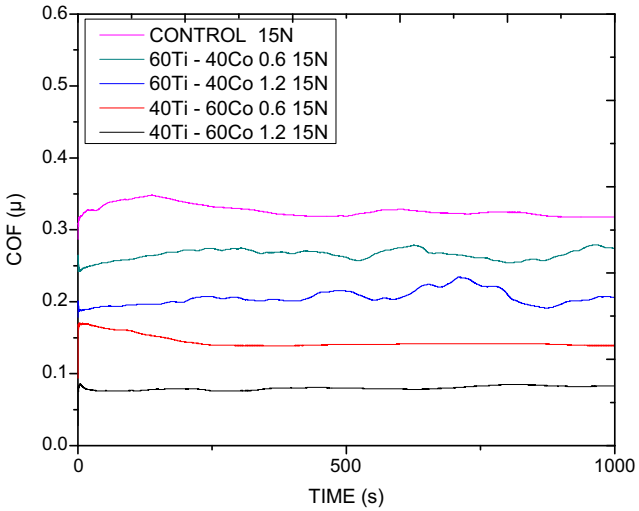

Fig. 19 Variation of coefficients of friction of Ti-Co coatings with sliding time

sliding wear test, contact regions influenced by high local temperature may lead to a rapidly reduced localized hardness of neighboring points on the coating. This reduction in hardness can result into severe plastic deformation mechanism leading to increased material removal. Thus, wear depth is more pronounced. This is in line with the works of Xue and Wang [33]. Figure 20 adheres to the direct proportionality between the coefficient of friction and wear depth during dry sliding wear test.

The communication between the clad surface and the counter body is addressed by the additional percentage of cobalt in the titanium matrix. As higher hardness characteristics are achieved by increased percentage of cobalt, the amount of soft matrix in interaction with the hard surface is effectively reduced, thus resulting into a corresponding reduction in wear depth. A governing law that explains this trend is the Archard's law [53] which states that wear

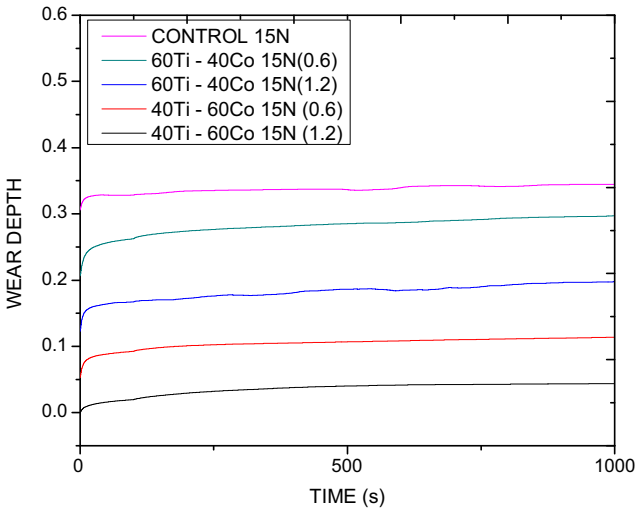

Fig. 20 Variation of wear depth of Ti-Co coatings with sliding time

property is inversely proportional to hardness. Zhang [54] stated that intermetallic compounds present support high hardness which is useful for high wear resistance.

4 Conclusion

In this study, the effect of laser scan speed on microstructural evolution and tribological properties of the clad samples were investigated. The admixed proportion of Ti-Co composition was also examined to evaluate and infer a decisive conclusion concerning the laser parameter. Therefore, the following conclusions are drawn from the work:

1. With the incorporation of the Ti-Co metallic coatings, the microstructure was reinforced and strengthened considering an increase scan speed and incorporation of higher amount of cobalt powder.
2. The microstructures of the 60Ti-40Co metallic coatings were characterized by flat polygonal dendrites with equal fractions of $CoTi_2$ eutectics at 0.6 m/min and needle-like (acicular) dendrites at 1.2 m/min while the coatings with higher percentage of cobalt proffered leaf-like structures within the coatings. Furthermore, an increase in laser scan speed resulted in an insufficient dendritic growth, yielding a solidification process dominated by nucleation rather than grain growth.
3. The Ti-Co metallic coatings were reinforced by hard intermetallic phases of $CoTi_2$, CoTi, $AlTi_2$, $AlCo_5$, $AlCo_2Ti$, and Al_2Ti at different compositions, resulting from the in situ chemical reaction in the molten pool. These intermetallic phases attributed to the improvement of the wear resistance. In addition, laser clad coating with high scan speed displayed better wear resistance of titanium alloy Ti6Al4V than that of low scan speed.
4. Friction coefficients were observed to be reduced with the incorporation of the metallic coatings. With increase in laser scan speed, the coefficients were reduced as a result of rapid solidification, formation of smaller strong grains and hard intermetallic phases within the coating. Net wear loss was greatly reduced as scan speed increased while the governing wear mechanism associated with the coating deposited at scan speed of 0.6 m/min were abrasive wear and plastic deformation while coating fabricated at 1.2 m/min was abrasive wear.

Funding information This research is supported by the Tshwane University of Technology, Pretoria, in collaboration with the National Laser Centre (NLC), Council of scientific and industrial research (CSIR), Pretoria, South Africa.

References

1. O. Adesina, P. Popoola, and O. Fatoba, Laser surface modification—a focus on the wear degradation of titanium alloy, 2016
2. Feng S-r, Tang H-b, Zhang S-q, Wang H-m (2012) Microstructure and wear resistance of laser clad TiB–TiC/TiNi–Ti2Ni intermetallic coating on titanium alloy. Transactions Nonferrous Metals Soc China 22:1667–1673, 7//
3. Banerjee D, Williams JC (2013) Perspectives on titanium science and technology. Acta Materialia 61:844–879, 2//
4. Weng F, Yu H, Chen C, Liu J, Zhao L, Dai J (2016) Microstructure and property of composite coatings on titanium alloy deposited by laser cladding with Co42+TiN mixed powders. J Alloys Compounds 686:74–81, 11/25/
5. Bansal DG, Eryilmaz OL, Blau PJ (2011) Surface engineering to improve the durability and lubricity of Ti–6Al–4V alloy. Wear 271: 2006–2015, 7/29/
6. Garbacz H, Wieciński P, Ossowski M, Ortore MG, Wierzchoń T, Kurzydłowski KJ (2008) Surface engineering techniques used for improving the mechanical and tribological properties of the Ti6A14V alloy. Surface Coatings Technol 202:2453–2457, 2/25/
7. Chikarakara E, Naher S, Brabazon D (2012) High speed laser surface modification of Ti–6Al–4V. Surface Coatings Technol 206: 3223–3229, 3/15/
8. Popoola API, Loto CA, Osifuye CO, Aigbodion VS, Popoola OM (2016) Corrosion and wear properties of Ni-Sn-P ternary deposits on mild steel via electroless method. Alexandria Engineering J 55: 2901–2908, 9//
9. Obadele BA, Andrews A, Olubambi PA, Mathew MT, Pityana S (2015) Effect of ZrO2 addition on the dry sliding wear behavior of laser clad Ti6Al4V alloy. Wear 328–329:295–300, 4/15/
10. Fu Y, Zhang X-C, Sui J-F, Tu S-T, Xuan F-Z, Wang Z-D (2015) Microstructure and wear resistance of one-step in situ synthesized TiN/Al composite coatings on Ti6Al4V alloy by a laser nitriding process. Optics Laser Technol 67:78–85, 4//
11. Mu M, Liang J, Zhou X, Xiao Q (2013) One-step preparation of TiO2/MoS2 composite coating on Ti6Al4V alloy by plasma electrolytic oxidation and its tribological properties. Surface Coatings Technol 214:124–130, 1/15/
12. Yilbas BS, Hashmi MSJ, Shuja SZ (2001) Laser treatment and PVD TiN coating of Ti-6Al-4V alloy. Surface Coatings Technol 140: 244–250, 6/1/
13. Zhang J, Xue Q, Li S (2013) Microstructure and corrosion behavior of TiC/Ti(CN)/TiN multilayer CVD coatings on high strength steels. Appl Surface Sci 280:626–631, 9/1/
14. Adebiyi DI, Popoola API (2015) Mitigation of abrasive wear damage of Ti–6Al–4V by laser surface alloying. Materials Design 74: 67–75, 6/5/
15. Savalani MM, Ng CC, Li QH, Man HC (2012) In situ formation of titanium carbide using titanium and carbon-nanotube powders by laser cladding. Appl Surface Sci 258:3173–3177, 1/15/
16. J. Dutta Majumdar and I. Manna, 21—laser surface engineering of titanium and its alloys for improved wear, corrosion and high-temperature oxidation resistance. In: Waugh, J. L.G. (ed). Laser Surface Engineering. Woodhead Publishing, 2015, pp. 483–521
17. Ion JC (2005) Chapter 12—cladding. In: Ion JC (ed) Laser Processing of Engineering Materials. Butterworth-Heinemann, Oxford, pp 296–326
18. Li HC, Wang DG, Chen CZ, Weng F (2015) Effect of CeO2 and Y2O3 on microstructure, bioactivity and degradability of laser cladding CaO–SiO2 coating on titanium alloy. Colloids Surfaces B: Biointerfaces 127:15–21, 3/1/
19. Paydas H, Mertens A, Carrus R, Lecomte-Beckers J, Tchoufang Tchuindjang J (2015) Laser cladding as repair technology for Ti–6Al–4V alloy: influence of building strategy on microstructure and hardness. Materials Design 85:497–510, 11/15/
20. Wu C, Ma M, Liu W, Zhong M, Zhang H, Zhang W (2009) Laser cladding in situ carbide particle reinforced Fe-based composite coatings with rare earth oxide addition. J Rare Earths 27:997–1002, 12//
21. Yang J, Liu F, Miao X, Yang F (2012) Influence of laser cladding process on the magnetic properties of WC–FeNiCr metal–matrix composite coatings. J Materials Processing Technol 212:1862–1868, 9//
22. Cai F, Jiang C, Fu P, Ji V (2015) Effects of Co contents on the microstructures and properties of electrodeposited NiCo? Al composite coatings. Appl Surface Sci 324:482–489, 1/1/
23. Gao L-l, Bian X-f, Tian Y-s, Fu C-x (2009) Effect of Co on microstructure and interfacial properties of Fe-based laser cladding. J Iron Steel Res, Int 16:84–88, 7//
24. Langelier BC, Esmaeili S (2009) in situ laser-fabrication and characterization of TiC-containing Ti–Co composite on pure Ti substrate. J Alloys Compounds 482:246–252, 8/12/
25. Xue Y, Wang HM (2005) Microstructure and wear properties of laser clad TiCo/Ti2Co intermetallic coatings on titanium alloy. Appl Surface Sci 243:278–286, 4/30/
26. Alemohammad H, Esmaeili S, Toyserkani E (2007) Deposition of Co–Ti alloy on mild steel substrate using laser cladding. Materials Sci Engineering: A 456:156–161, 5/15/
27. Amine T, Newkirk JW, Liou F (2014) Investigation of effect of process parameters on multilayer builds by direct metal deposition. Applied Thermal Engineering 73:500–511, 12/5/
28. Telasang G, Dutta Majumdar J, Padmanabham G, Tak M, Manna I (2014) Effect of laser parameters on microstructure and hardness of laser clad and tempered AISI H13 tool steel. Surface Coatings Technol 258:1108–1118, 11/15/
29. Mahamood RM, Akinlabi ET (2015) Effect of laser power and powder flow rate on the wear resistance behaviour of laser metal deposited TiC/Ti6Al4 V composites. Materials Today: Proceedings 2:2679–2686
30. Liu X-B, Yu R-L (2009) Influences of precursor constitution and processing speed on microstructure and wear behavior during laser clad composite coatings on γ-TiAl intermetallic alloy. Materials Design 30:391–397, 2//
31. Sun G, Tong Z, Fang X, Liu X, Ni Z, Zhang W (2016) Effect of scanning speeds on microstructure and wear behavior of laser-processed NiCr–Cr3C2–MoS2–CeO2 on 38CrMoAl steel. Optics Laser Technol 77:80–90, 3//
32. Dutta Majumdar J, Manna I, Kumar A, Bhargava P, Nath AK (2009) Direct laser cladding of Co on Ti–6Al–4V with a compositionally graded interface. J Materials Processing Technol 209: 2237–2243, 3/1/
33. Xue Y, Wang HM (2009) Microstructure and dry sliding wear resistance of CoTi intermetallic alloy. Intermetallics 17:89–97, 3//
34. Zhu Y, Chen X, Zou J, Yang H (2016) Sliding wear of selective laser melting processed Ti6Al4V under boundary lubrication conditions. Wear 368–369:485–495, 12/15/
35. Obadele BA, Masuku ZH, Olubambi PA (2012) Turbula mixing characteristics of carbide powders and its influence on laser processing of stainless steel composite coatings. Powder Technol 230: 169–182, 11//
36. Adesina OS, Mthisi A, Popoola API (2016) The effect of laser based synthesized Ti-Co coating on microstructure and mechanical properties of Ti6al4v alloy. Procedia Manufacturing 7:46–52
37. Mahamood RM, Akinlabi ET, Shukla M, Pityana S (2013) Scanning velocity influence on microstructure, microhardness and wear resistance performance of laser deposited Ti6Al4V/TiC composite. Materials Design 50:656–666, 9//

38. Shuja SZ, Yilbas BS (2011) Laser produced melt pool: influence of laser intensity parameter on flow field in melt pool. Optics Laser Technol 43:767–775, 6//
39. Davydov AV, Kattner UR, Josell D, Waterstrat RM, Boettinger WJ, Blendell JE et al (2001) Determination of the CoTi congruent melting point and thermodynamic reassessment of the Co-Ti system. Metall Mater Trans A 32:2175–2186
40. Weng F, Yu H, Chen C, Dai J (2015) Microstructures and wear properties of laser cladding Co-based composite coatings on Ti–6Al–4V. Mater Des 80:174–181
41. Meng Q, Geng L, Ni D (2005) Laser cladding NiCoCrAlY coating on Ti-6Al-4V. Materials Letters 59:2774–2777, 9//
42. Weng F, Chen C, Yu H (2014) Research status of laser cladding on titanium and its alloys: a review. Materials Design 58:412–425, 6//
43. de Damborenea J (1998) Surface modification of metals by high power lasers. Surface Coatings Technol 100–101:377–382, 3//
44. Gordani GR, ShojaRazavi R, Hashemi SH, Isfahani ARN (2008) Laser surface alloying of an electroless Ni–P coating with Al-356 substrate. Optics Lasers Engineering 46:550–557, 7//
45. Rotella G, Alfano M, Candamano S (2015) Surface modification of Ti6Al4V alloy by pulsed Yb-laser irradiation for enhanced adhesive bonding. CIRP Ann Manuf Technol 64:527–530
46. Fatoba OS, Popoola API, Aigbodion VS (2016) Experimental study of hardness values and corrosion behaviour of laser alloyed Zn-Sn-Ti coatings of UNS G10150 mild steel. J Alloys Compounds 658:248–254, 2/15/
47. Emamian A, Corbin SF, Khajepour A (2011) The influence of combined laser parameters on in situ formed TiC morphology during laser cladding. Surface Coatings Technol 206:124–131, 10/15/
48. Li J, Yu Z, Wang H (2011) Wear behaviors of an (TiB + TiC)/Ti composite coating fabricated on Ti6Al4V by laser cladding. Thin Solid Films 519:4804–4808, 5/31/
49. Ma Q, Li Y, Wang J, Liu K (2015) Investigation on cored-eutectic structure in Ni60/WC composite coatings fabricated by wide-band laser cladding. J Alloys Compounds 645:151–157, 10/5/
50. Cai B, Tan Y-f, Tu Y-q, Wang X-l, Tan H (2011) Tribological properties of Ni-base alloy composite coating modified by both graphite and TiC particles. Transactions Nonferrous Metals Soc China 21:2426–2432, 11//
51. Zhang Y, Qu J, Wang H (2016) Wear characteristics of metallic counterparts under elliptical-locus ultrasonic vibration. Appl Sci 6:289
52. Guo C, Zhou J, Yu Y, Wang L, Zhou H, Chen J (2012) Microstructure and tribological properties of Ti–Cu intermetallic compound coating. Materials Design 36:482–489, 4//
53. Ali D, Butt MZ (2015) The inverse Hall-Petch effect in Nd:YAG laser irradiated nickel. Materials Today: Proceedings 2:5302–5307
54. Zhang L, Wang C, Han L, Dong C (2017) Influence of laser power on microstructure and properties of laser clad Co-based amorphous composite coatings. Surfaces Interfaces 6:18–23, 3//